Structural and magnetic properties of Mn_5Ge_3 clusters in a dilute magnetic germanium matrix

C. Bihler,[a] C. Jaeger, T. Vallaitis,[b] M. Gjukic, and M. S. Brandt
Walter Schottky Institut, Technische Universität München, Am Coulombwall 3, 85748 Garching, Germany

E. Pippel, J. Woltersdorf, and U. Gösele
Max-Planck-Institut für Mikrostrukturphysik, Weinberg 2, 06120 Halle, Germany

(Received 17 October 2005; accepted 17 February 2006; published online 15 March 2006)

We have characterized the structural and magnetic properties of low-temperature molecular-beam epitaxy grown Ge:Mn by means of high-resolution transmission electron microscopy (HR-TEM), energy dispersive x-ray spectroscopy, and superconducting quantum interference device (SQUID) magnetometry. We find a coherent incorporation of Mn_5Ge_3 clusters in an epitaxially grown Ge:Mn matrix, which shows the characteristics of a diluted magnetic semiconductor phase of Mn-doped Ge. The clusters are preferentially oriented with the hexagonal [0001] direction parallel to the [001] growth direction of the Ge:Mn matrix, as determined from both HR-TEM and SQUID measurements. © *2006 American Institute of Physics*. [DOI: 10.1063/1.2185448]

One major problem in realizing spintronic devices is the injection of spin-polarized charge carriers into nonmagnetic semiconductors. Dilute magnetic semiconductors (DMS) are one promising approach to this problem. So far, most research activity has focused on III/V DMS such as $Ga_{1-x}Mn_xAs$, with Curie temperatures as large as $T_C=172$ K.[1–3] Mn-doped Ge, which as a group-IV element would be compatible with silicon-based microelectronics, has been studied to a much lesser extent. The growth of DMS Mn_xGe_{1-x} layers was reported in 2002 by Park *et al.*[4] Since then, only a few further studies on Mn_xGe_{1-x} have been published.[5–9] This is probably caused by the fact that the growth of the DMS Mn_xGe_{1-x} is complicated by its tendency to form thermodynamically favorable ferromagnetic intermetallic precipitates, e.g., Mn_5Ge_3.[5,10–13] To gain further insight into the complex growth of this material system, we have performed a detailed structural and magnetic characterization of molecular-beam epitaxy grown Ge:Mn layers. From magnetization measurements via a superconducting quantum interference device (SQUID), the presence of Mn_5Ge_3 clusters is clearly evident. High-resolution transmission electron microscopy (HR-TEM) shows that the Mn_5Ge_3 clusters are coherently incorporated in a Mn_xGe_{1-x} DMS matrix with an average Mn concentration of about 2%.

The sample reported on here was grown by low-temperature molecular beam epitaxy (LT-MBE) on a semi-insulating Ge(001) substrate. The Mn effusion cell was calibrated by elastic recoil detection (ERD) analysis and energy dispersive x-ray spectroscopy (EDXS) measurements. The substrate was heated to 600 °C for 30 min in the MBE system prior to the deposition process. The 300 nm layer with an average composition of $Mn_{0.03}Ge_{0.97}$ determined from the Mn and Ge flux was grown with a rate of 1.0 Å/s and at a temperature of 225 °C, conditions known to favor formation of clusters.[6] For the TEM and HR-TEM analyses performed in cross section, the samples were thinned by the standard process including ion beam milling.

A TEM overview (Fig. 1) shows the existence of spherical to elongated clusters with a diameter of 10–15 nm. Apparently, the precipitation does not start immediately at the wafer epilayer interface. Also, the distribution of clusters throughout the epilayer is inhomogeneous. Within almost all of these clusters, we observe well defined moiré patterns that are a strong indication for precipitates that are monocrystalline and are embedded in a monocrystalline matrix. Furthermore, clusters appear to be preferentially oriented, as the moiré patterns of most clusters are parallel to the interface.

Figures 2(a) and 2(b) show HR-TEM images of the $Mn_{0.03}Ge_{0.97}$ epilayer with atomic resolution. The images are cross sections of the Ge(110) plane. The orientation of the wafer/epilayer interface is marked by dashed lines. The well resolved lattice planes extending throughout the whole image reflect the high crystalline quality of the epilayer. The calculated fast Fourier transformation (FFT) pattern of Fig. 2(a), shown in Fig. 2(d), can be understood with the help of the theoretical diffraction patterns shown in Fig. 2(c). The main features of the FFT pattern are very well reproduced by the diffraction pattern of Ge(110) [Fig. 2(c), left panel]. If one assumes an orientation of the hexagonal Mn_5Ge_3 phase ($a_{Mn_5Ge_3}=7.184$ Å, $c_{Mn_5Ge_3}=5.053$ Å) (Ref. 14) with

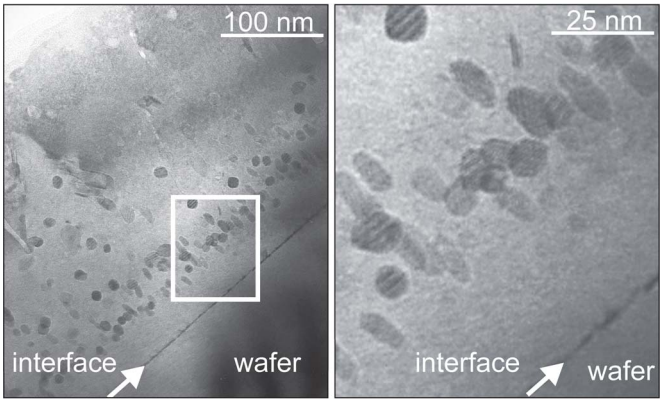

FIG. 1. TEM image of a $Mn_{0.03}Ge_{0.97}$ epilayer on a Ge wafer (left) with a magnified section (right). The arrows mark the interface between the wafer and epilayer.

[a]Electronic mail: bihler@wsi.tum.de
[b]Present address: Universität Karlsruhe, Engesserstr. 5, 76131 Karlsruhe, Germany.

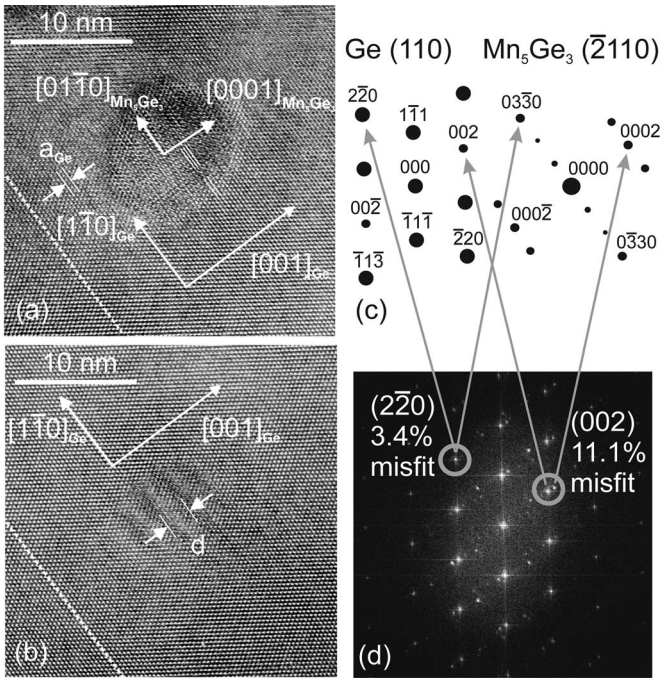

FIG. 2. (a) and (b) HR-TEM images of typical clusters in $Mn_{0.03}Ge_{0.97}$. The orientation of the wafer-layer interface is marked by dashed lines. (c) Standard diffraction patterns of Ge(110) and $Mn_5Ge_3(\bar{2}110)$. (d) Calculated FFT pattern of (a).

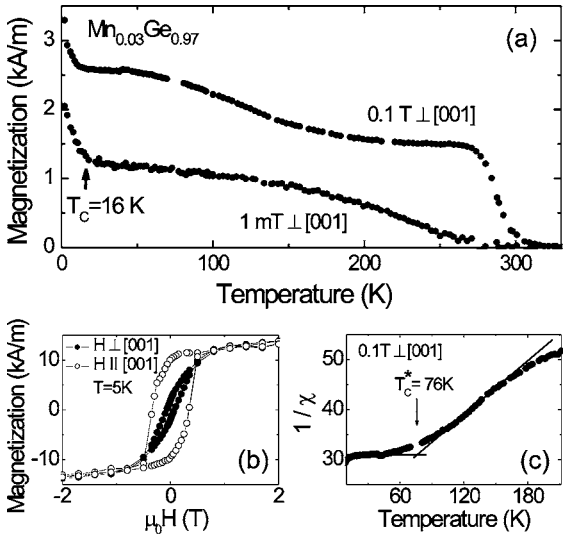

FIG. 3. Temperature dependence of the magnetization measured at 1 mT and 0.1 T for the magnetic field oriented in the epilayer. (b) Hysteresis loops at $T=5$ K for the magnetic field oriented in (•) and perpendicular to (◦) the layer. (c) Curie-Weiss plot measured at 0.1 T for the magnetic field oriented in the epilayer.

$[0001]_{Mn_5Ge_3}||[001]_{Ge}$ and $[\bar{2}110]_{Mn_5Ge_3}||[110]_{Ge}$ for the cluster in Fig. 2(a), the corresponding diffraction pattern [Fig. 2(c), right panel] together with that of Ge(110) very well reproduces the FFT pattern. The lattice mismatch of 3.4% between $[03\bar{3}0]_{Mn_5Ge_3}$ and $[2\bar{2}0]_{Ge}$ parallel to the surface is apparently compensated by a homogeneous distortion (only one reflex is visible for both $[2\bar{2}0]_{Ge}$ and $[03\bar{3}0]_{Mn_5Ge_3}$). This is not possible any more for the much larger lattice mismatch of 11.1% between $[0001]_{Mn_5Ge_3}$ and $[001]_{Ge}$ in growth direction, where two separate diffraction reflexes for $[002]_{Ge}$ and $[0002]_{Mn_5Ge_3}$ are identifiable. Therefore, the corresponding interface has to be semicoherent and has to exhibit misfit dislocations, which as a matter of fact are visible via tracking the progression of the atomic layers as indicated by the lattice planes in Fig. 2(a). Further evidence for a mismatch of 11.1% is provided by the cluster shown in Fig. 2(b). In this image, the geometric cluster to matrix relation gives rise to a pronounced moiré pattern parallel to Ge[001]. With $a_{Ge}=5.658$ Å, a period of 2.4 nm for the moiré pattern is expected, which is in good agreement with $d=2.1$ nm observed experimentally in Fig. 2(b) particularly, as a possible superposition of homogeneous and periodic lattice strain caused by the interaction of the growth partners should be taken into consideration.[15]

Zeng *et al.*[13] grew epitaxial Mn_5Ge_3 films on Ge(111) substrates and found an epitaxial relationship of $[0001]_{Mn_5Ge_3}||[111]_{Ge}$ with $[\bar{2}110]_{Mn_5Ge_3}||[1\bar{1}0]_{Ge}$. The lattice mismatch between successive lattice planes of $[0001]_{Mn_5Ge_3}$ and $[111]_{Ge}$ is 29%. This large value does not cause any problems in growth direction. However, for growth on a Ge(001) substrate—as in our case—epitaxial growth would be complicated considerably. The alignment of $Mn_5Ge_3(0001)||Ge(001)$ we determined from HR-TEM above seems to be energetically more favorable for Mn_5Ge_3 clusters incorporated in a Ge:Mn matrix because of the lower mismatch of 11.1%. Nevertheless, we would like to point out that for the epitaxy relation determined above there also is a mismatch of 11.4% between $[\bar{2}110]_{Mn_5Ge_3}$ and $[110]_{Ge}$ perpendicular to the HR-TEM cross section in Fig. 2(a), probably leading to further dislocations.

Additional spatially resolved EDXS measurements performed in the scanning mode of the TEM showed an approximately constant Mn concentration $x\approx0.02$ within the matrix and an increased Mn concentration within the clusters. A quantitative determination of the Mn concentration in the cluster is difficult due to the superposition of the cluster and the surrounding matrix also giving rise to the moiré pattern. The fact that the clusters are only observed after the growth of about 50 nm of Ge:Mn with 2% Mn suggests that the formation of Mn_5Ge_3 clusters at the growth temperature of 225 °C can only occur when a large enough amount of Mn is accumulated at the growth front. When this is the case, homogeneous nucleation sets in at a well defined distance from the interface. Mn_5Ge_3 precipitates are also found throughout the whole remainder of the layer.

Further evidence for the existence of a Mn_5Ge_3 phase is provided by the magnetization measurements shown in Fig. 3(a). The temperature dependent magnetization was measured for external fields of $\mu_0H=1$ mT and 0.1 T oriented in the epilayer. The measurement perfomed at low field clearly shows the presence of two magnetic phases. We attribute the steep increase of magnetization below 16 K to a DMS formed by Mn atoms incorporated substitutionally in the Ge matrix, which will be discussed in more detail later. The transition temperature of the second magnetic phase $T_C\approx290$ K corresponds to the value $T_C=296$ K reported for the intermetallic compound Mn_5Ge_3.[16] The $M(H)$ hysteresis loops in Fig. 3(b) show a more pronounced rectangular shape when $H||[001]$. This indicates the presence of magnetic anisotropy with the easy magnetic axis in the out-of-plane direction and the hard axis in plane. According to our TEM analysis, the easy out-of-plane direction corresponds to the hexagonal [0001] direction of the majority of the Mn_5Ge_3

clusters. This is in agreement with Tawara *et al.*,[17] who found the magnetic easy axis to lie along the hexagonal [0001] direction of Mn_5Ge_3 single crystals. The deviation of the hysteresis curves in Fig. 3(b) from a rectangular shape even for the magnetic field oriented along this easy direction can be due to the variation of the preferential orientation of the clusters. In the epitaxial ferromagnetic Mn_5Ge_3 layers on Ge(111) surfaces investigated by Zeng *et al.*,[13] the magnetic easy axis is in the hexagonal basal plane. However, the authors state their samples being dominated by shape anisotropy, which in our case can be neglected because of the near-circular shape of the clusters.

For the magnetization measurements in a higher external magnetic field ($\mu_0 H = 0.1$ T) we observe the appearance of an additional shoulder below 200 K. Following the analysis of Li *et al.*,[6] we deduce a critical temperature of $T_C^* = 76$ K from the Curie-Weiss plot in Fig. 3(c). We attribute the strong increase of magnetization below 300 K for the measurement in the higher external field to a higher fraction of magnetic moments of the Mn_5Ge_3 clusters aligned along this magnetic hard direction.

A steep increase of magnetization at low temperatures in combination with the appearance of a concave shoulder in higher magnetic fields has already been observed by Li *et al.*[6] for Mn_xGe_{1-x} and is thought to be characteristic for a DMS based on the model of bound magnetic polarons (BMPs).[18,19] The transition temperatures of $T_C = 16$ K and $T_C^* = 76$ K of the sample studied here are in agreement with the values obtained by Li *et al.*[6] for material with similar Mn concentration of 2% in the DMS. However, for a more profound assignment to BMPs, a more detailed analysis including ac susceptibility measurements would be required, which lies beyond the scope of this paper. Here we can only state that from the temperature dependence of magnetization our material behaves quite similar to the published behavior.

Ferromagnetic clusters in a Mn-doped semiconductor matrix have already been investigated in detail.[20,21] MnAs clusters in GaAs:Mn grow with an epitaxial relationship of $(0001)\mathrm{MnAs}\,||\,(1\bar{1}1)\mathrm{GaAs}$ and $(01\bar{1}1)\mathrm{MnAs}\,||\,(002)\mathrm{GaAs}$ irrespective of the substrate orientation. In these clusters, the magnetic hard axis is along the [0001] axis of the MnAs clusters in contrast to the Mn_5Ge_3 case. The benefit of the Mn_5Ge_3 clusters discussed here could be the fact that the Ge:Mn DMS matrix becomes ferromagnetic (FM) while the GaAs:Mn matrix obtained by metalorganic vapor-phase epitaxy stays paramagnetic (PM) also at low temperatures. Therefore, an additional degree of freedom for spin-dependent transport through a cluster system embedded in a FM or PM matrix depending on temperature or Mn concentration is obtained.[22]

In conclusion, we have investigated the incorporation of ferromagnetic Mn_5Ge_3 clusters in a Ge:Mn matrix. The clusters were found to be preferentially oriented with their hexagonal [0001] direction aligned in the [001] growth direction of the $Mn_{0.03}Ge_{0.97}$ layer. This assignment is confirmed by magnetization measurements, which show that the magnetic easy axis of the epilayer is out of plane, in agreement with reports of an easy magnetization of bulk Mn_5Ge_3 in the hexagonal [0001] direction.

The work at the Walter Schottky Institut was supported by Deutsche Forschungsgemeinschaft through SFB 631. Discussions with S.T.B. Goennenwein and the possibility to perform SQUID measurements at the Walther-Meissner-Institut are gratefully acknowledged.

[1] D. Chiba, K. Takamura, F. Matsukura, and H. Ohno, Appl. Phys. Lett. **82**, 3020 (2003).
[2] K. W. Edmonds, P. Boguslawski, K. Wang, R. Campion, S. N. Novikov, N. R. S. Farley, B. L. Gallagher, C. T. Foxon, M. Sawicki, T. Dietl, M. Buongiorno Nardelli, and J. Bernholc, Phys. Rev. Lett. **92**, 037201 (2004).
[3] A. Nazmul, S. Sugahara, and M. Tanaka, Phys. Rev. B **67**, 241308 (2003).
[4] Y. D. Park, A. T. Hanbicki, S. C. Erwin, C. S. Hellberg, J. M. Sullivan, J. E. Mattson, T. F. Ambrose, A. Wilson, G. Spanos, and B. T. Jonker, Science **295**, 651 (2002).
[5] J.- S. Kang, G. Kim, S. C. Wi, S. S. Lee, S. Choi, S. Cho, S. W. Han, K. H. Kim, H. J. Song, H. J. Shin, A. Sekiyama, S. Kasai, S. Suga, and B. I. Min, Phys. Rev. Lett. **94**, 147202 (2005).
[6] A. P. Li, J. Shen, J. R. Thompson, and H. H. Weitering, Appl. Phys. Lett. **86**, 152507 (2005).
[7] S. Picozzi, L. Ottaviano, M. Passacantando, G. Profeta, A. Continenza, F. Priolo, M. Kim, and A. Freeman, Appl. Phys. Lett. **86**, 062501 (2005).
[8] O. Kazakova, J. Kulkarni, J. Holmes, and S. Demokritov, Phys. Rev. B **72**, 094415 (2005).
[9] S. Yu, T. Anh, Y. Ihm, D. Kim, H. Kim, S. Oh, C. Kim, and H. Ryu, Solid State Commun. **134**, 641 (2005).
[10] T. B. Massalski, *Binary Alloy Phase Diagrams*, (American Society for Metals, Metals Park, OH, 1986), vol. 2.
[11] T. Miyoshi, T. Matsui, H. Tsuda, H. Mabuchi, and K. Morii, J. Appl. Phys. **85**, 5372 (1999).
[12] Y. D. Park, A. Wilson, A. T. Hanbicki, J. E. Mattson, T. Ambrose, G. Spanos, and B. T. Jonker, Appl. Phys. Lett. **78**, 2739 (2001).
[13] C. Zeng, S. C. Erwin, L. C. Feldman, A. P. Li, R. Jin, Y. Song, J. R. Thompson, and H. H. Weitering, Appl. Phys. Lett. **83**, 5002 (2003).
[14] J. Forsyth and P. Brown, J. Phys. Condens. Matter **2**, 2713 (1990).
[15] J. van der Merwe, J. Woltersdorf, and W. Jesser, Mater. Sci. Eng. **81**, 1 (1986).
[16] N. Yamada, J. Phys. Soc. Jpn. **59**, 273 (1990).
[17] Y. Tawara and K. Sato, J. Phys. Soc. Jpn. **18**, 773 (1963).
[18] A. Kaminski and S. Das Sarma, Phys. Rev. Lett. **88**, 247202 (2002).
[19] A. Kaminski and S. Das Sarma, Phys. Rev. B **68**, 235210 (2003).
[20] T. Hartmann, M. Lampalzer, P. Klar, W. Stolz, W. Heimbrodt, H.- A. Krug von Nidda, A. Loidl, and L. Svistov, Physica E (Amsterdam) **13**, 572 (2002).
[21] P. J. Wellmann, J. M. Garcia, J.- L. Feng, and P. M. Petroff, Appl. Phys. Lett. **71**, 2532 (1997).
[22] W. Heimbrodt, P. Klar, S. Ye, M. Lampalzer, C. Michel, S. Baranovskii, P. Thomas, and W. Stolz, J. Supercond. **Feb.**, 1 (2005).